A New Process for Fabricating Nonwoven Fibrous-Reinforced Elastomer Composites

M. EPSTEIN[1,*] and R. L. SHISHOO[2]

[1]Technical Research Centre of Finland VTT, Textile Laboratory, P.O. Box 635, SF-33101 Tampere, Finland and
[2]TEFO-Chalmers University of Technology, Box 5402, S-402 29 Goteborg, Sweden

SYNOPSIS

A new type of mold was developed and tested for structural reaction injection molding (SRIM) of elastomer composites having polymer matrices made from a mixture of two components. These mixtures had short pot lives and relatively high viscosity. Channel systems for polymer feeding and vacuum application were investigated. The mold cavity was provided with up to 24 polymer feeding holes and 38 vacuuming holes. The cavity and channels were made from transparent materials that allowed easy observation and video recording of the polymer matrix flow. In addition, some design parameters were studied such as channel layout. Investigations were carried out on the mechanism of polymer matrix flow and fiber breakage during the formation of fiber-reinforced composites made of nonwoven fiber reinforcement structures with considerably longer fiber lengths than reported earlier. Other studies included determination of the effects of fiber type, fiber dimensions, and fiber/matrix v/v ratio on the matrix flow during impregnation. © 1992 John Wiley & Sons, Inc.

1. INTRODUCTION

Structural reaction injection molding (SRIM) is usually used to produce stiff composites containing polyester or epoxy matrices. In such techniques, the mold consists of a cavity that can be subjected to vacuum. The fiber-reinforcement structure in the form of mats or fabrics are placed into this cavity prior to applying vacuum followed by injecting the two-component polymer. Vacuum, sometimes in combination with pressure, is used to introduce the polymer into the mold cavity and to force it to penetrate the fiber-reinforcement structure and form the polymer matrix. For elastomer composite formation, this molding concept is new. The mold development was made because of the higher viscosity in typical two-component elastomers compared to normal polyester or epoxy-based rigid matrix polymers.[1-3]

Short-fiber reinforcement for elastomers has lately gained importance due to some processing advantages and improvements in the mechanical properties of the resulting products. Fiber-related variables that affect the properties include content of fiber, dispersion, orientation, and fiber length.[4,5] Short staple fibers are less effective as reinforcing material in low modulus materials than are rigid materials.[4,6-8] Being the continuous phase of the composite, the matrix must act not only as a protective encapsulant or binder for the fibers but also as the stress transfer medium between the applied force and the discontinuous reinforcing fibers.[4,7,9,10]

Many standard textile fiber materials such as cotton, rayon, nylon, and polyester have been used for the reinforcement of elastomers, especially for natural rubber. Other fiber materials used include glass, aramids, steel, and carbon. Shredded textile waste has also been used as reinforcement medium.[6,11]

The high viscosity of commonly used elastomers create problems in introducing textile staple fibers to elastomer composites, especially when conventional elastomer processing methods are used.[5,6] One major drawback in the fiber reinforcement of rubber-based elastomer composites has been the difficulty in introducing fibers of lengths longer than only a few millimeters in randomly dispersed directions into the matrix. The high viscosity of rubber com-

* To whom correspondence should be addressed.

Journal of Applied Polymer Science, Vol. 45, 1693–1704 (1992)
 CCC 0021-8995/92/101693-12$04.00

pounds requires the use of very large forces when mixing the fibers into such matrices. This results in a high frequency of fiber breakage with subsequent loss of reinforcement potential of the fibers.[4] The only way to incorporate longer fibers has been to laminate them in the form of fiber strands such as cords or fabrics between layers of rubber compounds.

The aim of the present work was partly to develop better techniques for fabricating elastomer-based fiber-reinforced composites with longer fibers and partly to investigate the conditions that allow better mixing and distribution of fibers in the matrix. The latter aim required investigations on polymer matrix flow during formation of fiber-reinforced elastomer composites.

2. EXPERIMENTAL

2.1. Description of the Experimental Molds

The general idea was to build an SRIM mold with a cavity to produce flat composite samples for testing. A reinforcement fiber structure was introduced into the mold cavity prior to injection of the polymer matrix. The requirements for the mold were as follows:

i. The ability to form sample plates for testing.
ii. The ability to satisfactorily impregnate reinforcement fiber mats.
iii. The ability to achieve uniform polymer matrix distribution into the entire sample plate.

The mold was developed in order to distribute the polymer matrix uniformly into the cavity through several equidistant feeding holes. An exploded view of the mold is shown in Figure 1. The mold consisted of two main units: the channel unit and the cavity unit, which were placed on top of each other.

The main feature of the mold was the channel design that consisted of two separate systems: one for the polymer and one for the vacuum. The channels were designed to provide the shortest possible way from the polymer and vacuum inlet holes to the polymer feeding and vacuum holes, respectively, in the cavity. The feeding holes were distributed symmetrically with respect to the center lines of the mold cavity and equidistantially with respect to each other. The channel unit consisted of three plates: the top plate, the channel plate, and the stabilization plate. The channel plate was a rubber plate with the channels cut as v-grooves. The feeding holes were perforated on appropriate places from the channels through the rubber plate.

From Figure 2 it is seen that the channels of the polymer and vacuum channel systems cross each other, which made it necessary to place them on opposite sides of the channel plate. The polymer channels were formed between the top plate and the v-grooves on one side of the channel plate. The vacuum channels were formed between the stabilization plate and the v-grooves in the channel plate on the opposite side from the polymer channels. The distances between the feeding holes were in the range between 40 and 50 mm, and the distance from feeding hole to nearest vacuum hole, between 27.5 and 32 mm. There were 4–6 surrounding vacuum holes

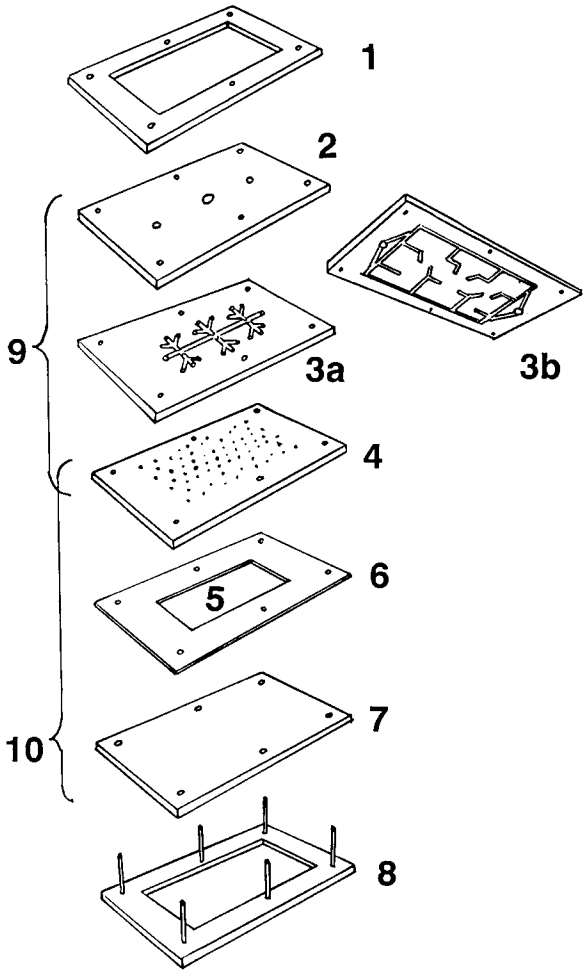

Figure 1 Exploded view of mold: (1) top support; (2) top plate; (3a) channel plate seen from polymer channel side; (3b) channel plate seen from vacuum channel side; (4) stabilization plate; (5) cavity; (6) frame plate; (7) bottom plate; (8) bottom support; (9) channel unit; (10) cavity unit.

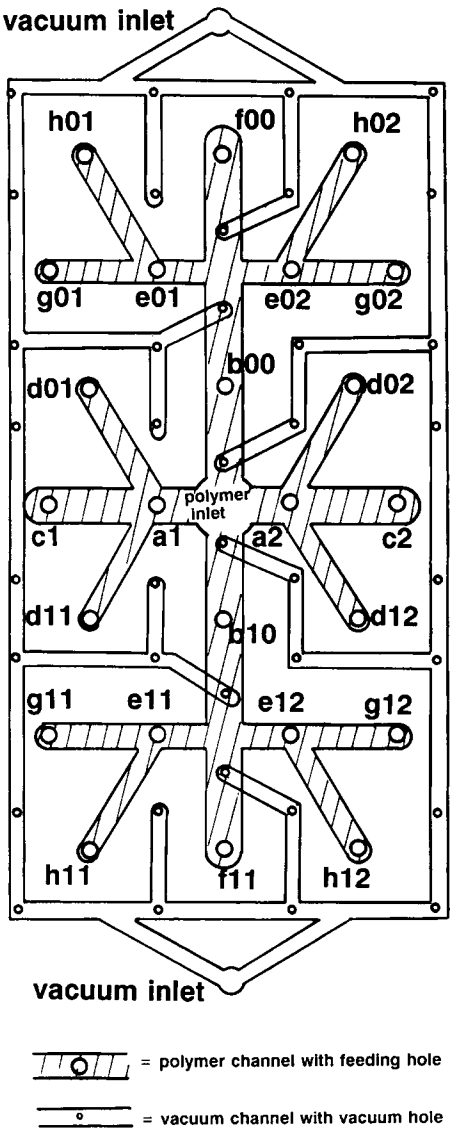

Figure 2 Chart of polymer and vacuum channel systems of the third mold (superimposed on top of each other). Hole category a and b: no bifurcations or bends after inlet hole; hole categories c–f: one bifurcation to previous hole and one channel bifurcation after inlet hole; hole categories g and h: two bifurcations to previous holes and two channel bifurcations after inlet hole.

for each feeding hole. The diameter of the feeding holes was 7.8 mm, and vacuum holes, 2.8 mm. The number of feeding holes was 24, and vacuum holes, 38.

The cavity unit consisted of the stabilization plate, the frame plate, and the bottom plate (Fig. 1). The stabilization plate was a polypropylene plate and was mounted below the channel plate. It formed the top side of the mold cavity and had holes that corresponded to the feeding holes and vacuum channels of the channel plate against which it was fitted. The cavity had a length of 315 mm and a width of 165 mm; its height, and thereby the thickness of the sample, was determined by the thickness of the frame plate (3–9 mm). The top and bottom plates were made of transparent acrylic material, which provided visibility of the cavity and the polymer channel systems. However, the vacuum channel system, which was located between the channel and the stabilization plates in the interior of the mold, was not visible.

The mold plates were clamped together and with bottom supports, resulting in a mold set. This was placed in horizontal position with mirrors positioned angularly for monitoring the elastomer flow in the cavity and channel systems simultaneously. Elastomeric polymer was fed to the inlet hole by pouring through a funnel/collar combination. The mold set, the mirrors, and the funnel together with the video camera formed a mold assembly (see Fig. 3).

2.2. Test Materials

2.2.1. Matrix Materials

The elastomeric matrix polymer consisted of a system (Baytech from Bayer Ag) where the polyol was a polyether compound containing small amounts of tertiary aliphatic amine and a primary aromatic diamine and with activator added. Its viscosity was measured to 3000 cP at 20°C. The isocyanate was a polyether–TDI prepolymer with isocyanate groups. Its viscosity was measured to 20,000 cP at 20°C, 3000 cP at 40°C, and 800 cP at 60°C. Their advantage in SRIM processing compared to many other elastomers is low viscosity; their disadvantage is rather short pot life (max. ca. 2 min).[12]

2.2.2. Fiber Reinforcements

As reinforcement, nonwoven mats of three basically different structures, needle-bonded, chemically bonded, and water-jet-bonded, were used. The fibers in the mats were polyester (PES), polypropylene (PP), acrylic (PAN), or *m*-aramid (Nomex). Each mat contained fibers of only single polymer type. Properties of the mats are listed in Table I.

2.3. Test Methods

The reinforcement fiber mats were tested for weight according to standard test method SFS 3192.[13] Thickness was measured using a Shirley thickness gauge according to standard test method SFS 3380.[14]

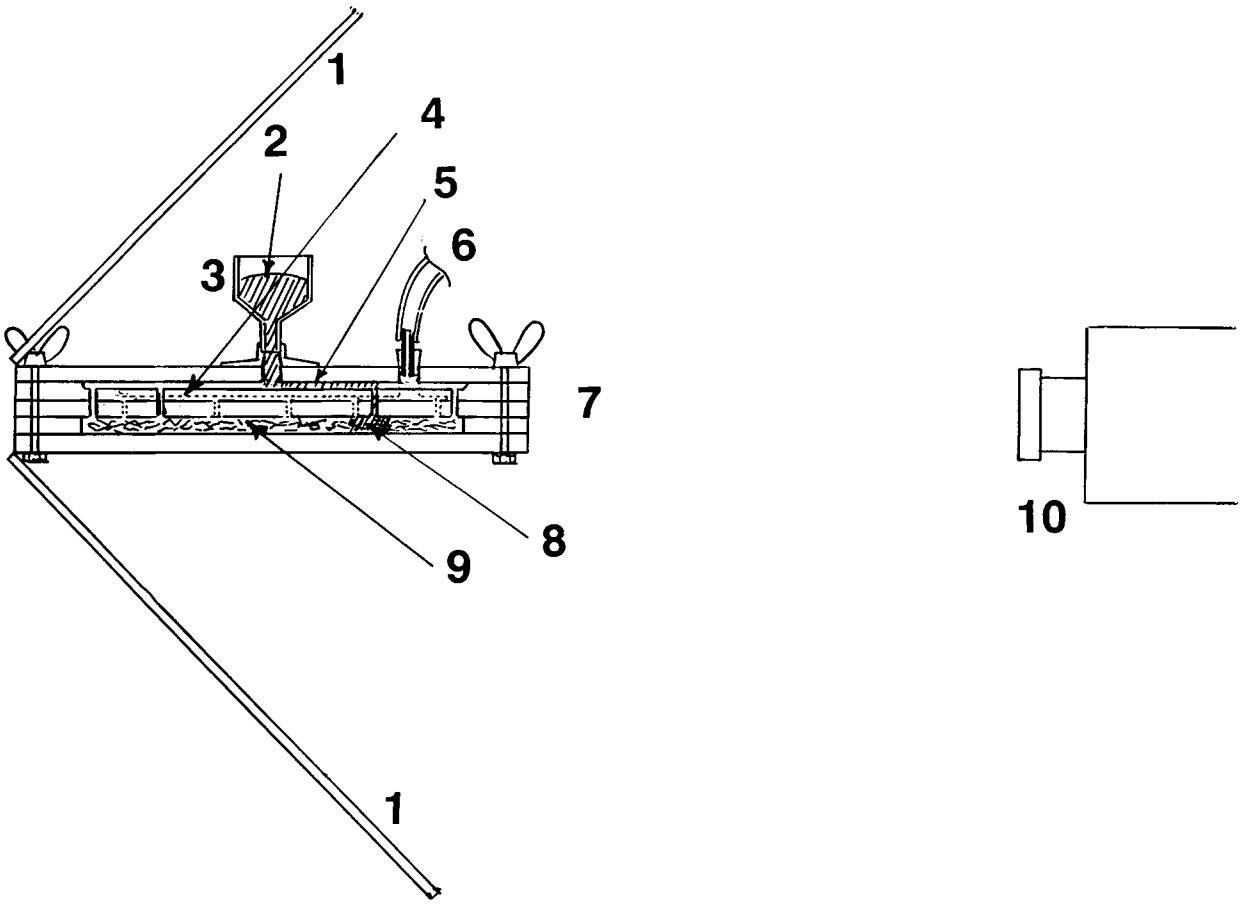

Figure 3 Mold assembly: (1) mirror; (2) polymer; (3) funnel; (4) vacuum channel; (5) polymer channel (polymer shown flowing through one channel and one feeding hole only); (6) vacuum connection; (7) mold set; (8) advancing matrix polymer; (9) reinforcement fiber mat; (10) video camera.

Inherent viscosity was measured using a Brookfield Model RVT viscosimeter.

The actual length of the fibers as present in the mats was tested by picking fibers out of the mat and laying them straight out on a fabric of black velvet and measuring the length. The average value of 10 fibers representing a population was calculated. The average value of the 10 fibers in each population was taken as the actual length of the fiber as present in the mat.

The length of fibers in the finished composite samples after preparation was tested by heating a 120 × 120 mm sample in a beaker with 100% purum acetic acid for several hours until the matrix had disintegrated completely. Thereafter, the remaining fiber mat was lifted out of the beaker, washed with water, and dried in an oven. The fiber lengths in the mat were analyzed by using the method described earlier.

The volume fraction of fiber in the composite was determined by weighing a flat composite sample of even thickness and known area. The weight of the contained fiber reinforcement was calculated from eq. (1); the weight fraction of fiber in the composite, from eq. (2); and the volume fraction of fiber in the composite, approximated from eq. (3):

$$w_f = \frac{bw_f}{A_c} \tag{1}$$

$$wf_f = \frac{w_f}{w_c \times 100}\,\% \tag{2}$$

$$vf_f = \frac{w_f \rho_m}{\rho_f}\,\% \tag{3}$$

where w_f is weight of reinforcement fiber; bw_f, weight of fiber mat; A_c, sample area; w_c, weight of composite

Table I Properties of Reinforcement Fiber Mats

Mat No.	No. Layers	Fiber: Type	Fiber: Fineness/ Length (dtex/ mm)	Fiber: Blend Ratio in Mat (% w/w)	Bonding Method	Weight (g/m^2)	Thickness (mm)	Mat No.
1	1	PES	4.4/100 6.6/64	50/50	Needle-punching	205	5.05	1
2	1	PP	3.9/60	100	Needle-punching	165	4.25	2
3	1	PAN	2.9/100 7.7/100	50/50	Needle-punching	117	4.15	3
4	1	PES	6.6/64	100	Needle-punching	205	5.25	4
5	1	*m*-Aramid	2.2/50 6/75	40/60	Needle-punching	165	4.80	5
			2.2/50			330	9.30	5
5	2		6/75					
			2.2/50			495	14.45	5
5	3		6/75					
8	1	PES	7.3/53	100	Chemical bonding	87	9.65	8
12	1	PES	1.6/38	100	Waterjet	46	0.90	12
14	1	PES	1.6/38	100	Waterjet	84	0.70	14
14	2		1.6/38			168	1.90	14
16	1	PES	3.4/60 4.4/60 6.7/60	45/10/45	Waterjet	116	13.50	16
16	2		3.4/60 4.4/60 6.7/60			232	28.10	16
16	3		3.4/60 4.4/60 6.7/60	45/10/45		348	41.70	16
16	4		3.4/60 4.4/60 6.7/60	45/10/45		464	52.20	16

sample; wf_f, weight fraction of fiber in composite; vf_f, volume fraction of fiber in composite; ρ_m, specific weight of matrix; and ρ_f, specific weight of fiber. The densities of the materials used are listed in Table II.

The polymer matrix flow during the resin injection process was recorded and monitored with a suitable video recording arrangement. The polymer matrix flow from two injection holes of the mold cavity was recorded separately.

The flow time was recorded as the time from the moment the polymer matrix was visible at the location of the injection hole until the moment when the polymer matrix flow ceased. The polymer matrix flow was judged to cease either because the polymer matrix portion merged with the matrix portion

Table II Specific Weights of Fiber and Matrix Materials

Material	Density (g/m^3)
Fibers	
Polyester	1.37
Nomex (*m*-aramid)	1.38
Acrylic	1.16
Polypropylene	0.9
Matrix	
Baytec	1.03

Sources—fibers: Reutlinger Fasertafel 1974, ITR, Reutlingen, Textilpraxis International; matrix: measurement from sample with no fiber reinforcement.

flowing from a neighboring hole or because the flow stopped without completely filling the mold.

The flow distance was measured from the diameter of the emerging circular polymer matrix portions as seen on the video screen. The flow distance was calculated from the equation

$$l = \frac{d_v b}{2 b_v} \tag{4}$$

where l is flow distance; d_v, diameter of circular polymer matrix portion measured on video screen; b_v, width of composite sample measured on video screen; and b, width of actual composite sample.

In general, the composite samples produced with ease of injection were judged to be of good quality. They exhibited an even distribution between fibers and matrix and none or very little residual air.

2.4. Study of Polymer Matrix Flow in the Channel System

Experiments were made by injecting polymer into the cavity with no reinforcement installed. The time when the polymer entered through each feeding hole was recorded with reference to the starting time of the injection. Figure 4 illustrates the order of polymer entrance into the cavity from the individual holes for a typical experiment. Table III lists the length of the channels from the polymer inlet to the respective feeding holes, the numbers of bends as well as bifurcations in the channels referring to Figure 2, and, furthermore, the average polymer flow times. The feeding holes shown in Figures 2 and 4 were grouped into categories (represented by letters a–g) depending on their distance from the polymer inlet hole and number of bends and bifurcations in the preceding channel. This categorizing was done because of the large number of holes and their unique placement in the mold.

2.5. Fabrication of the Composite Samples

The mat was installed in the cavity and the mold was closed by clamping the plates together. If the thickness of the layer of mats exceeded the height of the cavity, the mats were compressed to fit into the cavity. No fastening of the fiber mat to the mold was used.

In some preliminary experiments, the viscosity of polymer mixes of preheated polyol and isocyanate as a function of time at three temperatures (20, 40, and 60°C) was measured and recorded. Preliminary impregnation experiments in which the polymer had different temperatures were also made using the mats listed in Table I of polyester (No. 1) and polypropylene (No. 2) in order to establish the appropriate polymer matrix temperature.

For the main experiments, the polyol and isocyanate were heated in separate vessels to 60°C in an oven, placed in a desiccator at 48 kPa for a period of 10–15 min, followed by mixing polyol and isocyanate with laboratory stirrer for 45 s. The mixture was then poured into the feeding funnel of the mold followed by the application of vacuum. The flow of elastomeric polymer matrix into the mold was monitored through the transparent walls of the cavity. When the cavity was entirely filled or when the polymer ceased to flow into the cavity, the vacuum was discontinued. The sample was left in the cavity for more than 5 h at room temperature and was then removed from the mold. The flow of the elastomeric polymer matrix through the reinforcement fiber assembly in all experiments was recorded, and the flow distance as well as the flow time were determined according to methods described in Section 2.3., Test Methods.

Samples with weight fractions of fibrous material varying between 0 and 16.7%, calculated using eq. (1), were produced using the fiber mats listed in Table I. Volume fractions of fiber calculated using eq. (3) did not differ significantly from the weight fractions. This is because of the similarity of specific weights of fibers and matrix in these experiments. The variables studied are listed in Tables IV and V.

The lengths of fibers recovered from samples made with reinforcement mats of polyester (No. 16), polypropylene (No. 2), acrylic (No. 3), and *m*-aramid fibers (No. 5) were compared with lengths of fibers taken from corresponding unused mats of these fiber types. The numbers of the mats refer to Table I. Fiber length was measured according to the methods described in Section 2.3, Test Methods; the fineness was approximated by microscopic comparison with fibers of known fineness.

The effect of the thickness of the composite sam-

Table III Polymer Flow in Mold with 24 Inlet Holes

Channel Length (mm)	No. of Channel		Flow Time (s)
	Bends	Bifurcations	
24.5	2	2	0.04
44.0	2	2	0.34
64.0	2	3	0.50
74.5	3	2	1.34
111.5	3	3	3.27
130.0	2	3	2.88
151.0	3	4	(2.66)
162.5	4	4	5.38

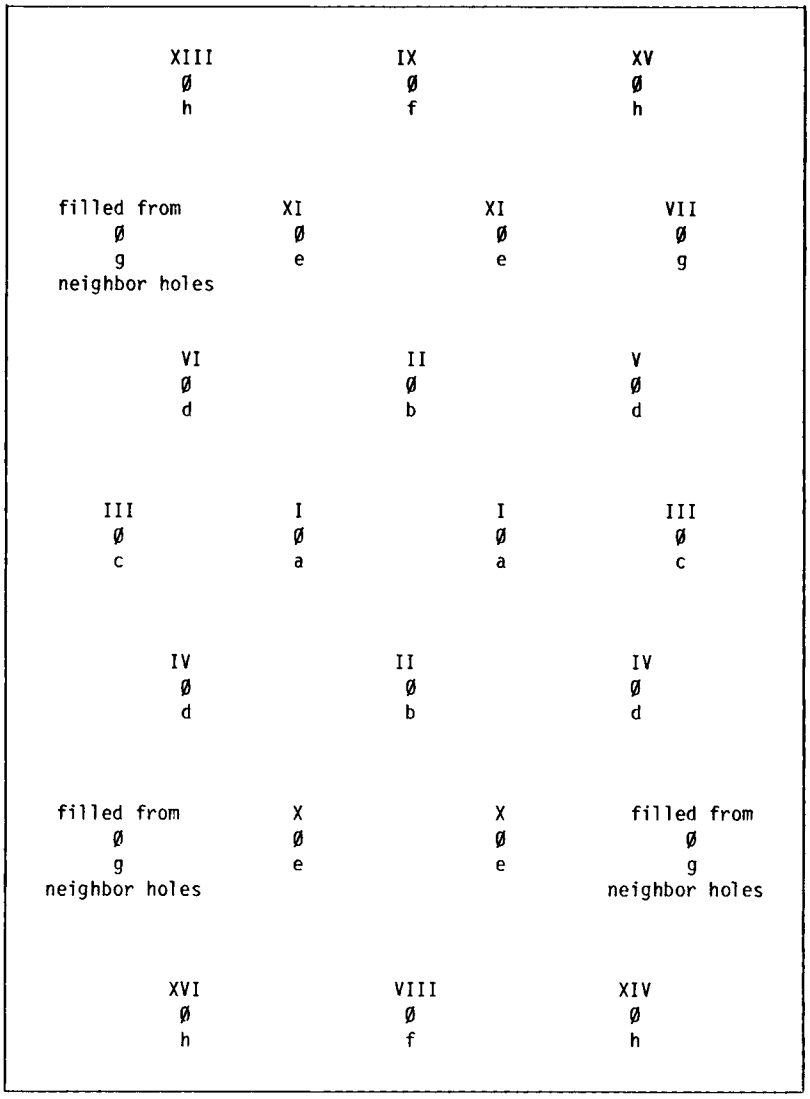

Figure 4 Chart of polymer injection sequence in mold; trials with no reinforcement installed. Roman numbers indicate order of polymer exit; letters, category of hole; ϕ, feeding hole.

ple was investigated using mat No. 16 (Table I) of a polyester fiber blend. The polymer was consecutively injected into one, two, and three layers of the mat in molds with 3, 6, and 9 mm cavity height, producing composite samples of corresponding thicknesses. The w/w fiber content was approximately 3.5% in all the experiments.

The influence of the fiber content was investigated by injecting polymer consecutively into one, two, and three layers of polyester fiber mat No. 16 (Table I) in a mold producing 3 mm-thick composite samples in all trials. The fiber content in the trials was 3.4, 6.5, and 10.1% w/w, respectively. The experiment was repeated using a mat of *m*-aramid fibers (No. 5, Table I), producing samples with fiber contents of 3.9 and 7.9%.

The maximum flow distance for the Baytech matrix polymer in polyester mat (No. 8, Table I) was tested by injection through one single hole (the other holes were closed) and monitoring and recording the spreading until it stopped.

3. RESULTS

3.1. Experience from the Mold

Figure 4 shows irregularities in the polymer flow to some holes (g). From these holes, no polymer flowed into the cavity so that the area close to them was impregnated from the surrounding holes. From Figure 2 it can be seen that the polymer flowing into the cavity from the neighbor holes (h and f) was

Table IV Conditions during Injection Experiments with Mats of Polyester and *m*-Aramid Fiber Arranged According to Increasing Weight of Reinforcement

Fiber Type	Weight of Reinforcement (g/m^2)	No. Layers	Mat No.	Fiber Content in Composite (Vol. Fraction %)	Flow time (s)	Flow Distance (mm)
PES	116	1	16	3.0	7.5	25.8
PES	232	2	16	5.9	60.0	17.5
PES	348	3	16	8.9	60.0	20.5
PES	464	4	16	11.9	60.0	16.0
m-Aramid	165	1	5	3.9	18.1	21.6
m-Aramid	330	2	5	7.9	56.7	18.4

able to enter the vacuum channel through the nearest vacuum holes. This polymer blocked the vacuum access to the vacuum holes serving the g holes that showed no polymer flow. The correlation is good between polymer flow time and channel length, especially up to 120 mm, showing a correlation coefficient of 0.93. Also, the correlation between flow time and numbers of bends and bifurcations, respectively, in the channel is acceptable, showing correlation coefficients of 0.81 and 0.82, respectively.

Through the transparent bottom plate of the mold, the polymer matrix could be seen to flow from the feeding holes into the fiber mat in the form of a continuously broadening polymer matrix body of practically circular shape. The polymer matrix advanced from the different feeding holes radially at similar rates and levels. During the impregnation, the mold was either filled up entirely so that the polymer matrix bodies emerging from the different feeding holes flowed together and merged or the polymer flow stopped before the mold got uniformly filled (Fig. 5).

No dislocation of the reinforcement fiber mat in the cavity could be observed during the matrix polymer injection process. The composite samples released very easily from the polypropylene surface, but acrylic surface needed thorough waxing to yield easy release. Stripping of the sample was made difficult because of the numerous feeding and vacuum holes.

3.2. Results from Impregnation Experiments

The length of the fibers recovered from composite samples reinforced with mats listed in Table I of polyester (No. 8), polypropylene (No. 2), acrylic (No. 3), and *m*-aramid (No. 5) as well as the lengths of the fibers from corresponding unused mats are listed in Table VI. This shows that no difference in fiber length could be noticed between fibers taken from raw mats and those taken from corresponding mats recovered from the elastomer composites.

Figure 6 shows the temperature dependence of the viscosity of the mixtures of polyether polyol and

Table V Conditions during Injection Experiments with Mats of Different Fiber Types Arranged According to Increasing Weight of Reinforcement

Weight of Reinforcement (g/m^2)	No. Layers	Mat No.	Fiber Content in Composite (Volume Fraction %)	Flow Time (s)	Flow Distance (mm)
116	1	16	3.0	7.5	25.8
117	1	3	3.3	6.2	24.5
165	1	2	6.1	6.3	26.3
165	1	5	3.9	18.1	21.6
205	1	1	5.2	19.4	22.5
232	2	16	5.9	60.0	17.5
240	3	14	6.2	32.0	
330	2	5	7.9	56.7	18.4
348	3	16	8.9	60.0	20.5
464	4	16	11.9	60.0	16.0

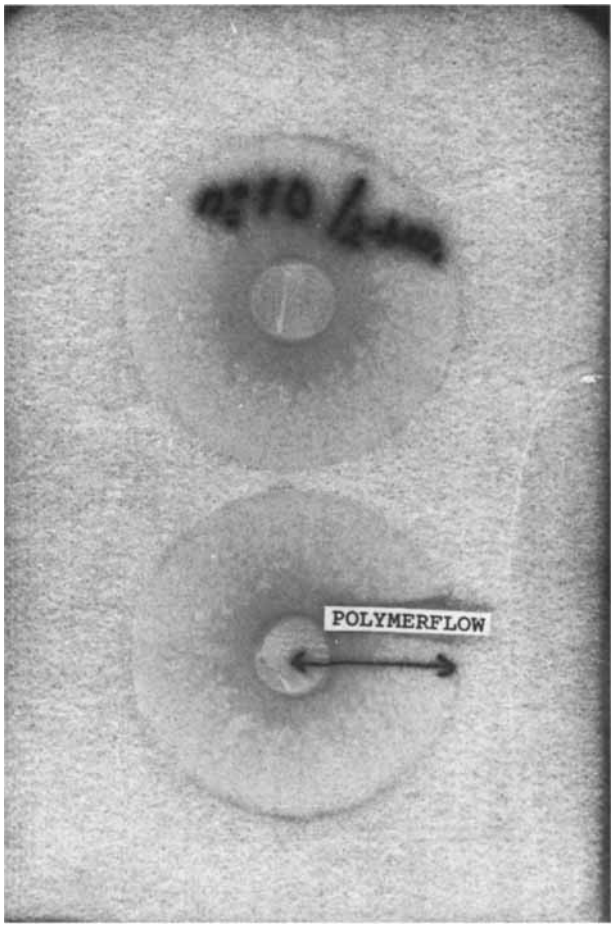

Figure 5 Polymer flow in SRIM; uncompletely filled mold.

polyether–TDI isocyanate. The viscosity of a mixture made from preheated polyol and isocyanate was found to stay lower compared with that of a mixture made from components at room temperature for 2 ½–3 min. The penetration of the polymer matrix into the reinforcement structure during the preliminary experiments was insufficient at room temperature, but improved when the viscosity of the polymer was lowered by heating the components before mixing.

The mold produced composite samples of 3–9 mm thickness with void-free matrix when using reinforcement fiber structures up to ca 200 g/m^2. However, for tighter fiber structures, the impregnation was inadequate in that the polymer matrix portions emerging from neighboring feeding holes stiffened before joining each other. The occurrence of voids was observed to increase for weight fractions above 5% w/w fibers; incomplete filling of the mold (totally nonimpregnated fiber mat areas) were observed between 10 and 16% w/w.

The dependence between polymer flow distance and flow time for different cavity heights and fiber contents, respectively, are shown in the time vs. flow curves in Figures 7 and 8. In a number of observations, the resin flow process could be divided into two different phases: an initial phase with rapid resin filling and a second phase with significantly lower filling velocity. In many experiments, the borders between the merging matrix polymer portions from neighboring feeding holes remained visible as shadowy lines that could be noticed during the formation of the composite. These lines, which remained visible in the finished sample, formed hexagons of almost equal sizes with the feeding hole in the center (the feeding holes near the cavity edge were surrounded by lines of other geometrical forms). The areas of the hexagons were of approximately identical size.

From the experiments using polyester fiber mat No. 16 (Table I) reported in Table IV and Figure 7, it is seen that there is a significant difference between the fiber contents 3.4 and 6.5% w/w as regards

Table VI Comparison of Length of Fibers Recovered from Composite Samples and from Unused Fiber Mats

	Dimensions of Fibers from Sample		Dimensions of Fibers from Mat	
Fiber Type	Length (mm)	Fineness (dtex)	Length (mm)	Fineness (dtex)
PES	49.7	7.3	50.7	7.3
PP	61.6	3.9	60.3	3.9
PAN	101.2	2.9	101.7	2.9
	100.3	7.7	103.6	7.7
m-Aramid	46.7	2.2	46.7	2.2
	71.9	6	72.4	6

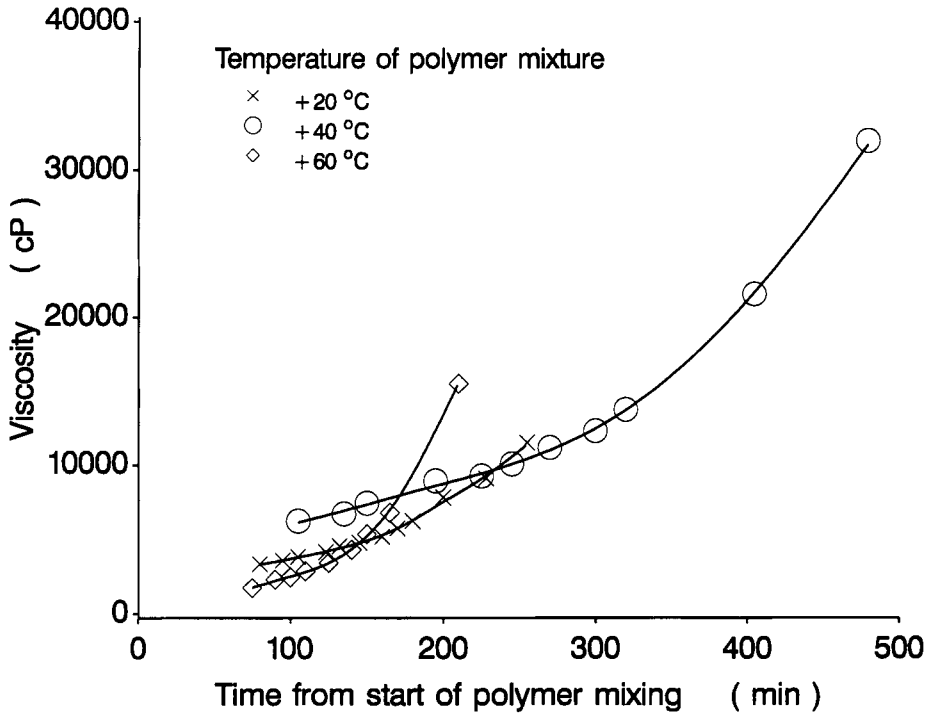

Figure 6 Viscosity development of polymer mix at different temperatures.

the rate of elastomeric polymer matrix flow. For weight ratios higher than 6.5% in our experiments, there is no further difference probably because of the limit of compactness reached in the samples. The experiments with *m*-aramid fiber mat reported in the same table indicate similar trends. Neither the number of layers nor the thickness of the composite sample has influence on the polymer matrix flow velocity with constant fiber content w/w, as seen in Figure 8.

In Table V, the test results for flow time and flow distance for the experiments with polyester, poly-

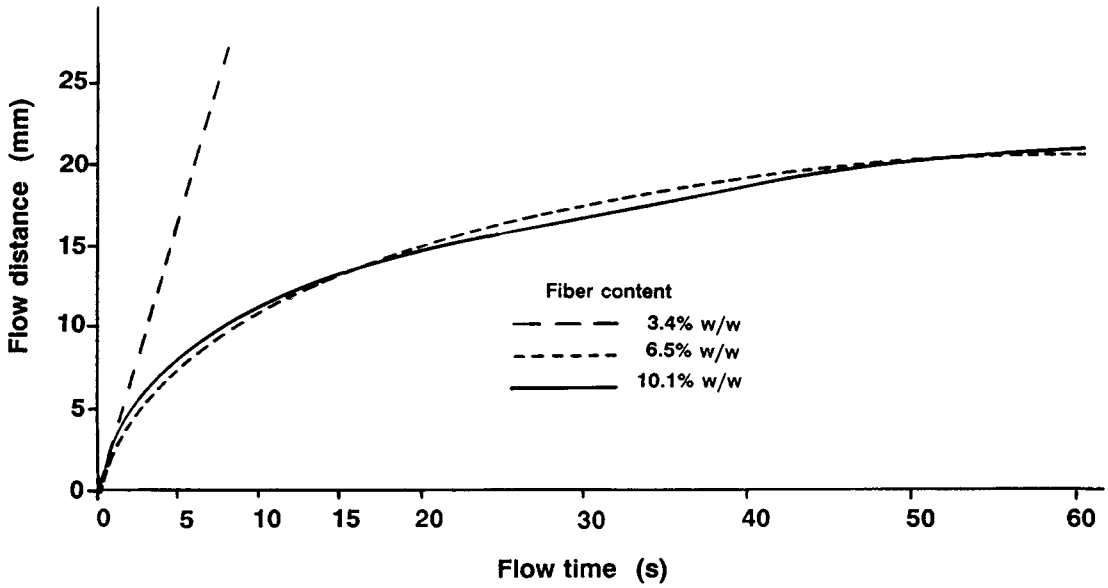

Figure 7 Polymer flow in SRIM; difference in number of mat layers and fiber content; composite thickness 3 mm.

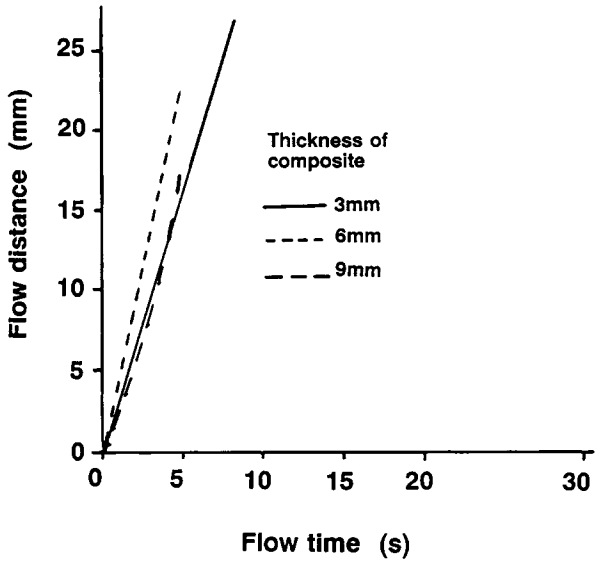

Figure 8 Polymer flow in SRIM; difference in thickness of composite and number of mat layers; fiber content 3.5% w/w.

propylene, acrylic, and *m*-aramide fiber mats are listed according to increasing fiber content and weight. There is rather good correlation between the fiber content of the composite and the flow distance of the polymer matrix: Furthermore, the fiber content and mat weight correlated rather well with the flow time of the polymer matrix; the correlation coefficients between the volume fraction of fiber and the flow time and flow distance were 0.79 and −0.72, respectively.

4. DISCUSSION

Our results using the SRIM procedure have shown that a channel distribution system in combination with equidistant multiple inlet holes facilitates the impregnation of reinforcement fiber structure with elastomeric polymer matrix. Symmetric arrangement of the channels gives a symmetric polymer flow into the cavity. This makes fastening of the reinforcement structure to the mold during resin injection unnecessary in order to prevent dislocation of the fiber mat inside the cavity.

If the polymer feeding holes are too far from each other, complete wetting and impregnation of the reinforcement fibrous structure becomes difficult to achieve. This is due to the polymer becoming too viscous for allowing penetration between the fibers until the polymer matrix portions from neighboring holes can merge with each other. The atmospheric pressure alone was not enough to force the matrix polymer through tight or thick reinforcement layers.

When using the SRIM technique, the spreading of elastomeric polymer matrix into the reinforcement structure improved when the viscosity was lowered by raising the temperature of the polymer. Knowledge of the interdependence between the viscosity of the mix of polyol and isocyanate and the temperature of the polyol and isocyanate prior to mixing proved important for the selection of suitable working parameters for the SRIM molding process.

No difference could be found between the length of fibers measured from the reinforcement fiber mats before and after fabrication of composites. This indicates that elastomer composites having randomly dispersed fibers can be made with relatively long staple fibers without damage.

The most important parameters affecting the matrix polymer injection dynamics in SRIM molding are the weight of the reinforcement mat and the volume fraction of fiber in the composite. The voids between the fibers vary in composites with different fiber contents. Higher fiber content gives smaller voids and, consequently, causes greater resistance to the polymer flow and reduction in its velocity. For a given fiber content, the dimensions of the voids between the fibers remain the same regardless of the thickness of the composite material, and, consequently, the velocity of the polymer flow is independent of the thickness. The areas inside the borderline hexagons surrounding the feeding holes did not vary, which indicates that the quantity of the matrix polymer injected through different feeding holes was nearly the same.

Good correlation could be obtained between fiber content and flow time as well as flow distance in these experiments using mats of four basically different types of fibers and also with mats bonded with three different methods. This shows that the fiber type or method of bonding is less important for the penetration of the polyurethane-based elastomeric matrix polymer than are fiber volume fraction and the weight of the reinforcement. The effects of fiber-surface properties has not yet been investigated as regards the effect on the elastomeric matrix polymer flow.

5. CONCLUSIONS

SRIM offers a suitable technique for making elastomer composites with fibers dispersed throughout the composite without damaging the fibers during the manufacturing process even when the fibers are

considerably longer than reported earlier in the literature.

The visibility offered by selecting glass or acrylic plates as mold material proved informative as to monitoring the formation of the composite samples in the molds. The transparent sides of the mold also enabled video recording of the formation, thereby making it possible to effectively monitor the filling sequences both of the mold cavity and the feeding channels.

Rubber proved to be a useful material for several parts of the mold, especially the feeding and vacuum channels and holes as well as for the edge walls of the cavity.

A number of polymer feeding and vacuum holes to the cavity facilitate the distribution of resin throughout the cavity of the mold. Symmetrically placed feeding and vacuum holes make securing of the fiber reinforcement mat to the mold unnecessary. Even complex resin channel systems give satisfactorily simultaneous resin distribution through all feeding holes. Because polymer that enters through the vacuum holes can block vacuum channels, it is important to design the vacuum channel system so that blockage by overflowing polymer is avoided. The arrangement of the feeding holes and adjacent vacuum holes in the mold design can be evaluated from video recordings of the resin travel in experiments with this type of mold.

Atmospheric pressure alone is not enough to force polymer into reinforcement structures containing fiber weight fractions exceeding 10%.

The polymer flow distance is inversely proportional and the flow time directly proportional to the fiber content and the weight of the reinforcement mat. The distance and velocity of polymer flow through the fiber mat increase when the viscosity of the polymer is lowered. Therefore, the temperature dependence of the viscosity of liquid elastomer matrix is an important criterion in the selection of optimal SRIM working parameters. The polymer flow may take place in two phases: a rapid phase in the beginning when most of the polymer enters the cavity, followed by a slower phase of polymer flow.

The influence of fiber surface properties and fiber distribution on the flow of elastomeric matrix polymer through different types of fiber mats needs to be studied in order to obtain a better understanding of the mechanism of matrix polymer impregnation.

This work was done at the Textile Laboratory of The Research Centre of Finland as part of their composites research program and under the guidance of Professor Roshan Shishoo of TEFO and Chalmers Technical University, Gothenburg, Sweden. I (M. Epstein) want to extend my gratitude to them for making this work possible.

REFERENCES

1. Anwendungstechnische Information, Merkblatt, Baytec Reparatur- und Giessmassen, Bayer PU/Anwendungstechnik Elastomere, Leverkusen, Germany, July 1987.
2. *Tuoteseloste G 300 Polyesterihartsi,* Neste Chemicals, Kulloo, Finland (technical brochure).
3. *SP 110 Epoxy Laminating System UK1102887-7,* Structural Polymer Systems Ltd., Coves, UK (technical brochure).
4. L. A. Goettler and K. S. Shen, *Rubber Chem. Technol.,* **56,** 619 (1983).
5. S. K. De and V. M. Murty, *Polym. Eng. Rev.,* **331,** 4 (1984).
6. A. P. Foldi, *Rubber World,* **196,** 19 (1987).
7. V. M. Murthy, A. K. Bhowmick, and S. K. De, *J. Mater. Sci.,* **17,** 709 (1982).
8. S. K. Chakraborty, D. K. Setua, and S. K. De, *Rubber Chem. Technol.,* **55,** 1286 (1982).
9. V. M. Murty and S. K. De, *J. Appl. Polym. Sci.,* **29,** 1355 (1984).
10. S. Akhtar, P. P. De, and S. K. De, *J. Appl. Polym. Sci.,* **32,** 5123 (1986).
11. Oy Nokia Ab, tekninen kumi, Elastomeerien mahdollisuuksia, Oy Nokia Ab, Tekninen Kumi, PL 20, 37101 Nokia, Finland (1985).
12. Anwendungstechnische Information, Merkblatt, Baytec Reparatur- und Giessmassen, Bayer PU/Anwendungstechnik Elastomere, Leverkusen, Germany, July 1987.
13. SFS-Käsikirja 27, Osa 1, 3 painos, Lokakuu 1987, Suomen Standardoimisliitto, Helsinki, Finland, SFS 3192 Tekstiilit. Tasomaistenneliömassan ja juoksumetrimassan määrittäminen (Textiles. Determination of mass per unit area and per unit length of textile fabrics), 1987.
14. SFS-Käsikirja 27, Osa 1, 3 painos, Lokakuu 1987, Suomen Standardoimisliitto, Helsinki, Finland, SFS 3380 Tekstiilit. Tasomaisten tuotteiden paksuuden määrittäminen (Textiles. Determination of thickness of textile fabrics), 1987.

Received July 17, 1991
Accepted October 10, 1991